AIAA JOURNAL
Vol. 34, No. 8, August 1996

Continuous Optical Discharge Stabilized by Gas Flow in Weakly Focused Laser Beam

R. Conrad*
U.S. Army Missile Research Development and Engineering Center, Redstone Arsenal, Alabama 35653
and
Yu. P. Raizer† and S. T. Sarzhikov‡
Russian Academy of Sciences, Moscow 117526, Russia

For the first time, an old experiment is described where a continuous optical discharge is maintained in a large, weakly focused beam of a gasdynamic CO_2-laser (P = 150 kW), the discharge being stabilized by nitrogen flow at a velocity of 10 m/s opposite to the plasma propagation. This experiment, in other words, produced a large, optical plasmotron. A detailed model, developed to simulate such phenomena numerically (including the laser supported combustion wave), is described. The most important factors, two-dimensional gas flow, heat conductivity, radiation heat exchange, and refraction of the laser radiation in the plasma, are taken into account. The numerical results for the aforementioned experiment are given, the temperature and velocity fields are plotted, and the gas energy balance is analyzed. The computed gas flow velocity (9 m/s) agrees well with the experimental value. For such a velocity, the numerical model shows that the plasma exists stably in a 150-kW beam at that section of the beam (a diameter of 3.2 cm) where the plasma was observed to stop in the experiment. On the basis of the developed theory (confirmed by comparison with the experiment and the numerical model), various other laser beam/plasma phenomena can be simulated; for example, the operation of a laser-plasma rocket thruster.

I. Introduction

IN a continuous optical discharge (COD) in gaseous media, a steady-state plasma is maintained by continuous laser radiation, usually from a CO_2 laser, although hydrogen fluoride (HF) and deuterium fluoride (DF) lasers have also been used. This effect was predicted theoretically in Ref. 1 and observed experimentally in Ref. 2. Then it was studied in a comprehensive way (see Refs. 3 and 4 and references therein).

There are three techniques generally used to produce CODs. Each requires that some initial ionization be produced to facilitate plasma formation. This may be done using an electric discharge of a source of ionizing radiation, or the laser beam itself can be used, by irradiating a solid target and creating some ionization near the target surface, by thermal ionization of vaporized target material.

Method 1 for production of CODs employs a fast optical focusing system to maintain the COD quasistationary, near the focus, in a quiescent gas. Very small movements of the COD may be produced by laser power variations or convective disturbance produced by the COD itself.

Method 2 uses a weakly focused laser beam in a quiescent gas a produce a COD near the focus, which moves at subsonic velocities toward the laser source. When the COD progresses to a point in the beam where the intensity is no longer sufficient to maintain it, it vanishes. This is usually followed immediately by ignition of another plasma. This type of COD was first observed in a pulsed Nd laser beam[5] and interpreted as a combustion process. It is thus sometimes referred to as a laser-supported combustion (LSC) wave.

Method 3 is a variation, albeit an important one, of method 2, in which a flow of gas is directed counter to the direction of propagation, at a velocity sufficient to bring the COD to a halt. By appropriate choice of gas flow velocity and test configuration, a stationary COD can be produced, in many different gases, irrespective of the speed of the optical system as long as the laser intensity is in excess of the COD maintenance threshold. The gas that passes through the COD is, of course, heated to very high temperatures, forming, in essence, a plasma jet. This type of plasma generator was suggested in Refs. 1 and 6 and referred to as an optical plasmotron (OP).

Aside from their purely scientific interest, the COD, LSC, and OP phenomena are important for several reasons involving the practical applications of laser technology. For example, the COD and OP can provide stable, localized, stationary plasmas in a number of gases, over a wide range of pressures. Since the plasma temperatures are very high compared with other kinds of discharges (viz., $\geq$20,000 K), they can be useful for spectroscopic and other kinds of investigations that require intense sources of radiation, particularly in the ultraviolet.

The COD and LSC phenomena frequently arise during materials processing, such as welding and cutting, where high laser intensities are used. Because these phenomena drastically change the nature of the radiation incident on the working surface, special procedures are sometimes required to prevent their formation.

Another possible application of these phenomena, in the field of space vehicle propulsion, is the laser thruster. This concept involves the generation of an OP in a suitable working gas, in a combustion chamber, with subsequent expansion of the heated gas through a supersonic nozzle. Such a thruster, theoretically capable of producing a very high specific impulse, has been studied both theoretically and experimentally in recent years.[7-13]

In 1971 the first of the authors performed an experiment that probably was the first experimental implementation of the OP scheme. The beam from a powerful gasdynamic, CW, CO_2 laser was focused on a metal target with low f-number optics. The plasma formed near the target surface and propagated up the laser beam. Simultaneously, a gas flow was directed coaxially in the direction of the laser radiation. At some distance from the target, the plasma stopped and continued to exist as long as the laser remained on. For a long time, the results of this experiment were not published (though they were mentioned in Ref. 14). Recently, however, restrictions on publication of the information were removed.

In recent years, the other two authors of this paper, without the benefit of the large-scale experimental data just mentioned, carried the theoretical studies of these phenomena far beyond the original work described in Refs. 1, 3, and 4. In addition to a more detailed and

Received June 30, 1993; revision received Aug. 11, 1995; accepted for publication Aug. 23, 1995.

*Supervisory Research Physicist, Weapon Sciences Directorate; currently Vice President, Conrad Consulting, Rf. 5, Box 355, Russellville, AL 35653.

†Professor and Head, Department of Physical Gasdynamics, Institute for Problems in Mechanics, 101 Vernadski Street.

‡Leading Researcher, Department of Physical Gasdynamics, Institute for Problems in Mechanics, 101 Vernadski Street.

sophisticated theoretical description, numerical models have been developed that simulate, with high resolution, the COD, LSC, and OP phenomena.[15–24]

All of the important factors that are of influence in these processes are taken into account, namely, radiative heat exchange, including radiation transfer in spectral lines; laser radiation refraction in the laser-sustained plasma (which can essentially change the light channel geometry and space distribution of the beam intensity); two-dimensional nature of the gas flow and the process as a whole (in which it can be seen in particular that the cold gas partially flows around the COD region and partially flows through it); and the possible vortex formation and convection arising under certain conditions due to gas heating and gravity.

Computations have been performed for comparison with various small-scale experimental studies. Good agreement has been obtained with the experimental data, and certain observed peculiarities of the phenomena have been explained. The large-scale experimental data, however, permit for the first time testing of certain critical underlying theoretical features that form the foundation of the numerical models, primarily in the area of radiative heat transfer.

In the present paper, agreement is obtained between measured and calculated velocities of the gas flow that causes the COD to stop at a certain section of the beam. This agreement makes it possible to replace many expensive experiments necessary for practical problems where the COD, LSC, and OP are used by numerical simulations. In what follows, we describe the experiments and their results, the main concepts of the theory and numerical simulation, the numerical results and the entire pattern of the stabilized COD flow, the temperature and flow fields, and the energy balance.

II. Experimental Scheme and Results

The experimental scheme is shown in Fig. 1. The laser was a large, CW, CO_2 gasdynamic laser, designed and built by the AVCO corporation. This device employed the processes of combustion of gaseous CO with subsequent expansion through a linear array of supersonic nozzles. A high-quality, TEM_{00} master oscillator beam of about 100 W was injected into the gain region just downstream of the nozzles. For the plasma experiments described here, a multipass, stable oscillator optical configuration was used. The beam was extracted through an aerodynamic window, using dry N_2 gas. A large gas diffuser downstream of the optical cavity performed pressure recovery to slightly above atmospheric pressure, permitting direct exhaust into the atmosphere.

The output power of the laser as configured for these experiments was 150 kW. Power was measured with a rotating, thin-blade reflector, which sampled the laser beam approximately 30 times per second and reflected 0.5% of the total beam power into a commercial, water-cooled calorimeter capable of handling up to 1 kW of continuous-wave (c.w.) power. Since the time constant of the calorimeter was about 0.5 s, this technique yields only a time-averaged power measurement.

Information on the time dependence of total power and intensity distribution was obtained using an EG and G scanning, infrared camera at up to 250 frames/s, viewing the diffuse reflection from the focusing mirror. Analysis of these data revealed a near-field intensity distribution resembling a skewed, distorted Gaussian with local variations of intensity of 30–50% in time intervals of 40–100 ms. Surprisingly, maximum total power variations were estimated at about ±10%.

The far-field intensity distribution was determined in separate experiments using burn impressions in Plexiglas® blocks. For the range of intensities used in these experiments, Plexiglas was found

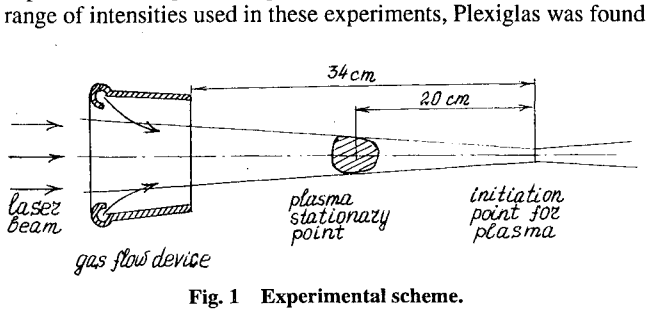

Fig. 1 Experimental scheme.

to ablate linearly, and if the irradiation time was short (less than a few seconds) and the depth/width ratio of the burn impression kept ≅1, the burn impression profile compared very well with time-averaged, infrared camera data. The far-field intensity distribution was Gaussianlike, with a peak/average ratio of 2.75. The beam radius and area were defined, as was the convention at that time, by the $1/e^2$ intensity contour.

The nominally collimated 10-cm-diam beam from the high-power laser was projected 60 m onto a 30-cm-diam, 8-m-focal length, spherical, uncooled mirror, fabricated from oxygen-free, high-conductivity (OFHC) copper. For laser run times of up to 20 s, mirror heating and distortion were not significant.

The gas-flow device shown in Fig. 1 consisted of a thin-wall, tapered, steel tube 30-cm long with a 10-cm diam at one end and a 7-cm diam at the other. A circular gas manifold fabricated from 0.5-in-diam copper tubing with numerous small holes spaced evenly around the circumference was brazed to the inside of the steel tube, just inside the larger diameter opening. The location of the holes was such as to direct the gas flow at an angle of about 30 deg to the inside wall of the steel tube. The manifold was connected to a bank of compressed gas bottles through a solenoid valve and regulator. This gas-flow device was crude and clearly would entrain ambient air into the gas flow. This would certainly cause experimental difficulties when using gases other than N_2 or air. For other gases, the intent was to place a material window over the entrance of the tube. Several such experiments were performed but were, for the most part, unsuccessful because of the inadequacies of the window materials. In any event, the gas-flow device operated well with N_2 gas, and the gas velocity field downstream of the exit port, as measured with a small, handheld pilot-tube, wind-speed meter, was both stable and reproducible.

The laser beam, referring again to Fig. 1, was reflected from the copper mirror, through the gas-flow device, and thence onto a metal plate target located at the focal point. Aluminum targets worked best, but steel and titanium were also successfully used for plasma initiation. Also used was a spark discharge between metal rod electrodes, driven by a repetitively pulsed, 300-kv Marx bank. This latter method of plasma initiation is preferred for making plasma spectroscopy measurements since contamination of the plasma environs with metal vapor is eliminated.

Trial and error were used to locate the optimum position for placing the gas-flow device. High-speed motion picture cameras operating at 1000 frames/s were used to determine the position and velocity of the plasma. The irradiated spot on the target had a radius $R_f = 1.4$ cm, producing an average radiation intensity on target $S_f = P/\pi R_f^2 = 24$ kW/cm^2. The plasma moved up the beam and stopped at a distance of 20 cm from the target. At that position, the beam radius was $R_0 = 1.6$ cm and the average intensity $S_0 = 18$ kW/cm^2. The velocity of the incident gas flow stabilizing the plasma was $\mu = 10$ m/s as determined from the position of the plasma relative to the exit port of the gas-flow device and the previously characterized gas velocity field.

III. System of Equations for Numerical Simulation

Consider the process of the plasma stabilized in a converging beam of the CO_2 laser when a cold gas flows in the direction of laser radiation propagation, the gas flow being incident on the plasma at a velocity u, as in Fig. 1, and the cool gas density being equal to ρ_0.

Since the problem in question is axisymmetric, we use the cylindrical coordinates (z, r). The z axis is directed along the gas flow in order for the axial velocity component V_z to be positive ($V_z = u$ and $V_r = 0$ at $z = -\infty$). The flow is subsonic, even in the high-temperature region, though the velocity there, V_z, is essentially greater than $u \sim 10$ m/s. For pressure $p_0 > 1$ atm, a gas can be considered to be in thermodynamical equilibrium. Since $p \approx \text{const} = p_0$, the gas dissociation and ionization depend on temperature T only. Neglecting the variations in the gas energy density due to small pressure variations (as well as viscous dissipation), we write the gas energy equation for the temperature:

$$\rho c_p \left(\frac{\partial T}{\partial t} + V \operatorname{grad} T \right) = \operatorname{div}(\lambda_r \operatorname{grad} T) + W - Q \qquad (1)$$

For $p \approx$ const, the gas density ρ is related to the temperature T. The heat conductivity λ_t, heat capacity c_p, and the viscosity are also functions of the temperature only. In addition to the summand describing the heat conductivity, there are terms corresponding to the energy release (in cubic centimeter per second) from laser energy absorption (W) and to the resulting rate of heat losses from heat radiation Q. Here Q is the difference between the rates of heat radiation emission and absorption.

The gas velocity V satisfies the continuity and momentum equations:

$$\frac{\partial \rho}{\partial t} + \operatorname{div} \rho V = 0 \tag{2}$$

For the momentum equation, one should use the Navier–Stokes equations, since the viscosity is of importance, especially in the case of high temperature.

As was shown when solving particular problems for LSC and OP, in many cases it would be reasonable to solve the equations using such variables as vortex and stream functions, rather than the natural variables V_z, V_r, p, and ρ. The point is that pressure variations in the Navier–Stokes equations are small, and therefore it is convenient to eliminate p from the gasdynamical equations. This can be done when differentiating the Navier–Stokes equations written for V_z and V_r. The equation obtained is reduced to the equation for curl $\bar{\omega} =$ rot V. When gas does not rotate around the axis ($V_\psi = 0$), the curl ω has only the azimuthal component $\omega = \omega_\psi$. In the steady-state case, the stream function $\Psi(z, r)$ coincides with the gas mass transfer rate through a circle of radius r at a section z (divided by 2π). We do not write here the rather cumbersome equations used to solve the problem of finding the flow pattern.

The heat sources distribution $W(z, r)$ depends not only on the laser beam attenuation due to its absorption but also on the beam refraction in the nonuniform plasma as well. It would be more correct to speak about self-refraction since the distributions of the electron density n_e (which determines the refraction index) and the heat sources are self-consistent. The importance of the refraction effect was emphasized in Refs. 19 and 25.

A mysterious (for a long time) observation was explained[18] by the refraction action. The COD plasma usually is shifted from an undistributed beam focus (geometrical focus) in the lens direction. If a laser is sufficiently powerful, the energy transmitted through a COD ought to be quite sufficient to initiate another COD at the geometrical focus where the radiation intensity is high. In reality, two plasma formations were never observed.

As the calculations[18,19] show, the plasma initiated in a focal region is shifted from this region toward the lens, together with the focus itself, i.e., in spite of the shift, the plasma remains localized in a region of the maximal laser radiation intensity. In the region of the maximum temperature, the beam ceases to converge due to refraction and becomes highly diverging, resulting in a beam of large cross section at the geometrical focus point. The minimum cross-sectional region, which is favorable to maintain plasma, coincides with a temperature peak region. The new radius of the beam at the geometrical focus appears to be almost an order of magnitude more than that for undisturbed beam focusing.

A beam passed through the COD region diverges with a significantly greater angle than in the convergence region. Of course, both these angles are the same if there is no plasma. This is shown graphically in Ref. 19. It is possible that the two temperature peaks in the COD obtained numerically in Ref. 13 can be explained by the fact that the refraction was not taken into account and therefore this calculation does not totally correspond to the real situation.

In our numerical models for the laser beam, refraction is computed according to the parabolic approximation of quasigeometrical optics. The beams are considered to be paraxial, whereas the radial distribution of the refraction index n and the absorption coefficient μ_ω are considered to be parabolic of the type

$$n(z, r) = n(z, 0) - [\alpha(z)]^2 r^2/2 \tag{3}$$

The parabolicity factor $\alpha(z)$ [which is of the order of the inverse effective radius of the light beam, $R(z)$] is approximately determined by the obtained radial distributions $n_e(z, r)$.

When considering the refraction effect in detail, we take into account the redistribution of the radiation intensity along a radius when the radiation propagates along the z axis. In a more simple model, the intensity radial distribution is considered to be Gaussian, but the function $R(z)$ is computed according to the refraction equation in Ref. 19, the energy release being taken as

$$W(r, z) = 2\mu_\omega P \exp\{-2r^2/[R(z)]^2\}/\{\pi[R(z)]^2\} \tag{4}$$

where $\mu_\omega \equiv \mu_\omega(z, 0)$ is the absorption coefficient on the axis and $P(z)$ is the laser beam power that decays approximately according to the equation

$$\frac{\partial P}{\partial z} = -\mu_\omega P \tag{5}$$

Here we do not consider the refraction in detail and do not write the equations (see Ref. 19) when considering the experiment in question, because such calculations are time consuming. Furthermore, when a beam is weakly diverging, the refraction effect is not as significant as in a case of sharp focusing. This was confirmed by test calculations. Therefore in Eq. (1), the undisturbed beam radius is taken as $R(z)$.

The absorption coefficient of the CO_2 laser radiation (when the second ionization of atoms is not taken into account) is given by the approximate formula[3]:

$$\mu_\omega = 11.7 p_e^2 (T/10^4)^{-\frac{7}{2}} g, \qquad g = 0.55 \ell_n 27 (T/10^4)^{\frac{4}{3}} p_e^{-\frac{1}{3}} \tag{6}$$

where μ_ω is expressed in cm^{-1} and T in degrees Kelvin. Here p_e (standard atmosphere) is the partial electron pressure.

By definition, the resulting energy losses due to emission and absorption of thermal radiation are

$$Q = \int_0^\infty æ_\lambda \int_{4\Omega} (I_{e,\lambda} - I_\lambda)\, d\Omega\, d\lambda = \int_0^\infty c\, æ_\lambda (U_{e\lambda} - U_\lambda)\, d\lambda \tag{7}$$

where $I_\lambda(r, z, \Omega)$ is the radiation intensity and λ is the radiation wave length, with the radiation being propagated in the Ω direction.

The equation $U_\lambda = c^{-1} \int_0^\infty I_\lambda\, d\lambda$ is the radiation density, the quantities $I_{e\lambda}$ and $U_{e\lambda}$ correspond to the equilibrium (Planck) state, and $æ_\lambda$ is the corrected spectral absorption coefficient, with stimulated emission taken into account. The case $Q < 0$ means that the gas in this region is heated by radiation. The intensity I_λ is governed by the radiation transport equation. When numerically stimulating COD, we use two models of the radiation heat exchange. One of them is based on the solution of the transport equation for I, in which all directions are divided into 7–19 angular parts. It is applied to consider the case of radiation transfer in spectral lines. To describe the radiation transfer in a continuous spectrum, the diffusion approximation is usually applied,[23] viz.,

$$-\operatorname{div}[(3\, æ_\omega)_{-1} \operatorname{grad} U_\lambda] = æ_\lambda (U_{e\lambda} - U_\lambda) \tag{8}$$

For the case of air, the entire real spectral range $\lambda = 0.02$–$4.0\ \mu m$ is divided, in the optimal way, into 10 different parts. In each part, the spectral coefficient $æ_\lambda$ is averaged. The losses and radiation heat exchange in atomic lines are not essential for the COD problem in air, as was confirmed by a special analysis.[19] Here the radiation transfer in spectral lines is not taken into account.

IV. Numerical Results and Discussion

The numerical experiment corresponds approximately to the real physical experiment. A converging light beam with a Gaussian intensity distribution along a radius is assumed. The CO_2 laser power is $P_0 = 150$ kW. The uniform flow of the cold air propagates in the direction of the incident laser radiation at $p_0 = 1$ atm and $T_0 = 300$ K. Although in the real experiments nitrogen is used, the air properties (for which the model was developed) differ from the nitrogen properties only slightly. In a narrow part of the converging beam the initial plasma region with temperature $T_{max} \approx 15000$ K is produced, and the plasma absorbs the laser radiation. The parts of the flow ahead of the plasma region are heated by heat conductivity and radiation and the high temperature front (the LSC wave) propagates to meet the laser beam. The cold gas velocity is chosen so as

to cause the wave to stop and the quasistationary COD to become stationary at a beam section with the same radius ($R_0 = 1.6$ cm) and the same average intensity of the undisturbed laser radiation (18 kW/cm^2) as in the physical experiment.

The cylindrical region for calculations is taken to be sufficiently large (30 cm along the axis and a diameter of 24 cm) that the boundary conditions have no influence on the numerical results. As a rule, the flow at the boundaries is considered to be undisturbed, with $T_0 = 300$ K. In choosing the size of a computed region we are limited by the computers available, since to obtain correct and reliable results, the computed region should be divided into sufficiently small cells. This is also a reason to assume an initial plasma region closer to the final position of the COD region than in the actual experiment. In the experiment, the plasma of the steady-state COD region moves 20 cm from the place of its initiation until it stops, whereas in the numerical experiment we take this distance to be equal to 10–12 cm. For the same reasons, the convergence angle is taken to be a little larger than in the experiment to stabilize the COD more rapidly. Otherwise, one should increase the computing region length. This should not influence the numerical results, since the variation of the undisturbed beam radius along the axial length of a temperature peak in the steady-state COD region appears to be small.

As the computation show, the plasma travels the distance between its initial and final positions in 25 ms. During the subsequent 320 ms of the computing time, the situation does not change, and so one can say that a stationary state is reached. The calculations indicate that the stationary state at the same beam section corresponding to the experiment is provided by an incident flow velocity $u = 9$ m/s, which agrees with the experimental value, $u = 10$ m/s.

The steady-state flow pattern is given in Figs. 2–6 where the flow and temperature fields are shown, as well as the plasma energy balance. The computed maximum temperature, $T_{max} = 14000$ K, is rather low as compared with the maximum temperature

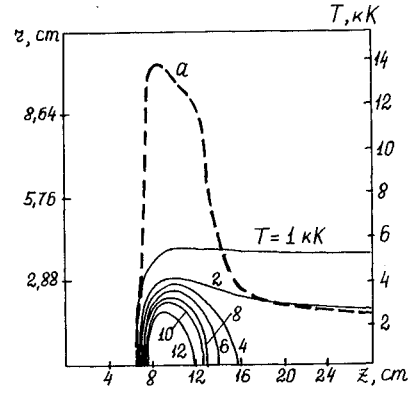

Fig. 2 Computed temperature field in a COD in air for $p = 1$ atm and gas-flow velocity $u = 9$ m/s, which provide a steady-state plasma in the beam section with the experimental diameter of 3.2 cm. The undisturbed laser radiation intensity is 1.8 kW/cm^2. The isothermal and temperature distributions (curve a) long the axial coordinate are given.

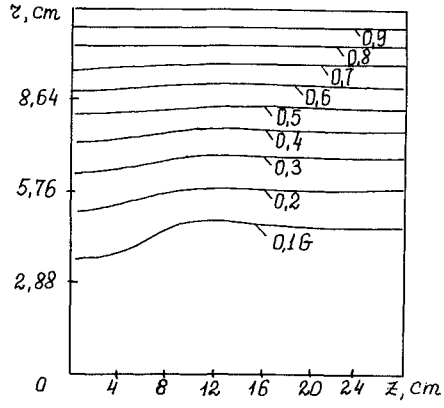

Fig. 3 Streamlines corresponding to a fixed fraction of the total flow rate $G = 7$ g/s.

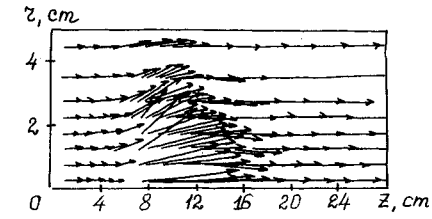

Fig. 4 Velocity field; the arrows show the velocity directions at a given point in space, the length of the arrow being proportional to the velocity magnitude.

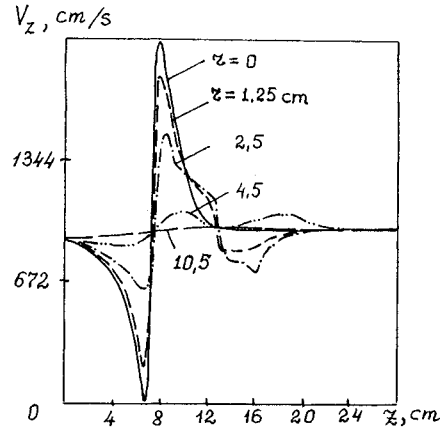

Fig. 5 Velocity distributions along the axial coordinates at various distances r from the axis. The minimum velocity corresponds to the velocity at which the nonheated gas inflows into a critical point of the high heated plasma body.

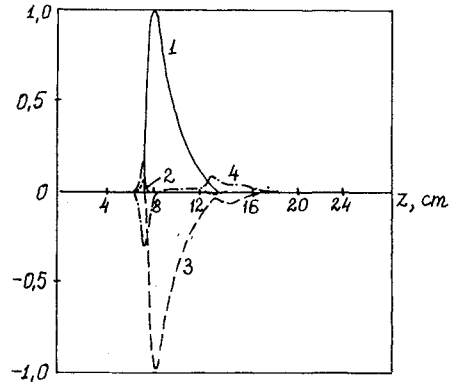

Fig. 6 Various constituents of the gas energy balance on the axis: 1—energy release in 1 cm^3/s due to absorption of the laser radiation, 2—energy taken away by the heat conductivity, 3—final losses due to the heat radiation (negative values correspond to dominant absorption of the heat radiation), 4—convective cooling, i.e., the energy practically spent to increase the enthalpy. All parameters are referred to 1 cm^3/s.

(17,000–18,000 K) measured in other experiments and obtained when computing other cases in the air (18,000 K). The major difference is that under the conditions considered here the laser power, beam radius, and plasma region's size are unusually large. The diameter of the region where $T \geq 1000$ K reaches 7 cm and the axial length is 5.5 cm. This causes the heat conductivity and radiation losses to be relatively small in comparison with the case of sharp focusing for not so powerful beams, where the sizes of a strongly heated region are from a few millimeters to 1 cm. To compensate for the relatively low losses (in the case of a large plasma region) it is sufficient to diminish the energy release density. This means a lower absorption coefficient and, as a result, a lower temperature.

The COD temperature front facing the incident laser radiation is very steep. The cold gas is heated by heat conductivity and radiation, their fluxes being directed forward to meet the laser radiation. The laser radiation absorption leads to very fast heating of the cold gas. This is seen in Fig. 6, where various components of the energy balance are given.

Behind the temperature front, the laser energy absorbed along the axis is lost mainly due to heat radiation. At the end of the COD region where a jet outflows from the region of laser radiation absorption, the temperature is not sufficient for significant heat radiation and the gas is cooled mainly by thermal expansion.

Using continuity equation (2) and that of the heat radiation transfer, one can represent the energy balance equation in a stationary case as

$$\mu_\omega P = \mathrm{div}(\rho \bar{V} w - \lambda_T \nabla T + \bar{S}), \qquad w = \int_0^T c_p a t \qquad (9)$$

where the first summand under the sign of div is the hydrodynamic energy flux (w is the specific enthalpy), the second one is the heat conductivity flux, and the third one corresponds to the heat radiation flux. All of these components of the energy balance are given in Fig. 6. The fact that the convective cooling (i.e., the first summand) near the plasma forefront dominates means that all absorbed laser energy is spent to increase the gas temperature.

A cold flow incident to the plasma at rest flows primarily around it, though a small fraction of the gas flow penetrates the highly heated region. The process of subsonic flow around a hot, low-density region ($\rho T \sim \rho_0 T_0$ due to $p = \mathrm{const}$) is similar to that around a solid body. This is confirmed by the exact analytical solution for the gas flow around a hollow sphere (in fact, a sphere of extremely low gas density).[22] The flowfield shown in Fig. 5 corresponds qualitatively to the results of the analytical model. When approaching a high-temperature region, that part of the flow that moves strictly along the axis decelerates by a factor of about $\sqrt{(\rho_0/\rho_m)} \sim 10$, where ρ_m is the minimum plasma density corresponding to $T_{\max}$. Penetrating to a highly heated zone, the gas flow accelerates by a factor of ρ_0/ρ_m, as compared with an axial velocity of the cold gas at a critical point of the heated sphere $u_{cr} = u\sqrt{(\rho_m/\rho_0)}$, or $\sqrt{(\rho_0/\rho_m)}$ times as compared with the velocity of the incident cold gas, u. As the gas is cooled, the gas jet outflowing from a heated region decelerates to the initial velocity u, far behind the heated region.

The gas mass fraction of order of $\sqrt{(\rho_m/\rho_0)}$, which is about 10% of the mass of the flow incident to a middle section of the sphere, penetrates into a heated hollow sphere. The rest of the gas mass (90%) flows around a hollow sphere as a solid body. All of these conclusions based on the analytical model are confirmed by numerical results shown in Fig. 5. Thus, the two-dimensional character of the flow in problems on the OP and LSC is a main factor in these processes, and the one-dimensional flow models used in many previous papers give a distorted flow pattern not representative of the real simulation. Suffice it to say that in a one-dimensional model the COD region is stabilized by the flow at a velocity u_1 that is $\sqrt{(\rho_0/\rho_m)} \sim 10$ times less than the real velocity u. According to the one-dimensional LSC model, in a tube from an open end, the wave propagates through free space at a velocity u_1, which is $\sqrt{(\rho_0/\rho_m)} \sim 10$ times less than the real velocity at which a bounded plasma region moves. If we assume the LSC to move through a tube from a closed end[3,22] its velocity is $\sqrt{(\rho_0/\rho_m)} \sim 10$ times greater than the real one. These results indicate that one-dimensional LSC and OP models fail.

V. Conclusions and Future Problems

The theory and numerical model presented here to describe the COD, LSC, and OP take into account the essential factors, namely, the two-dimensional nature of the flow, radiation heat exchange, and laser beam refraction in the laser-supported plasma. The results of the numerical simulation agree well with old (but only recently available) experimental results where a COD was maintained in a large beam from a very powerful CO_2 laser and was stabilized by the gas flow. This experiment can be considered as a prototype of an optical plasmatron. One of the most important problems requiring additional analysis, when modeling these phenomena numerically, is the problem of the stability, specifically, how to separate real unstable situations from instabilities due to imperfections of the numerical simulation. We came across this situation in particular when solving the described problem. For long simulated times ($t >$ 300–500 ms for the stationary state setting time of 25 ms), when the stationary flow seems to be reached, an instability arises and the solution slowly diverges. We believe that this is a result of counting region constraints and the forced, artificial character of the boundary conditions posed on the region boundaries. Because of continuous energy release, the gas is heated in the entire computational region. In reality, the heat is partially scattered in a surrounding space that is very large as compared with the plasma region size. The heat is absorbed partially by solid objects of high heat capacity, with slow convective flows being produced in the surrounding atmosphere. The problem of separating real, slow instabilities from those resulting from computational procedures seems to be very important when analyzing practical problems concerned with the COD, LSC, and OP, in particular, when analyzing laser thrusters where stable operation is of vital importance.

References

[1]Raizer, Y. P., "On the Possibility to Create a Light Plasmatrone and Power Required," *Zhurnal Eksperimenticheskoy i Teoreticheskoy Fiziki Pisma Redaktorovanie*, Vol. 11, 1970, p. 155.

[2]Generalov, N. A., Zimakov, V. P., Kozlov, G. I., Masyukov, V. A., and Raizer, Y. P., "Continuous Optical Discharge," *Zhurnal Eksperimenticheskoy i Teoreticheskoy Fiziki Pisma Redaktorovanie*, Vol. 11, 1970, p. 44y.

[3]Raizer, Y. P., "Laser-Induced Discharge Phenomena," Consultants Bureau, NY, 1977.

[4]Raizer, Y. P., "Optical Discharges," *Uspekhi Fizicheskikh Nauk*, Vol. 132, 1980, p. 549.

[5]Bunkin, F. V., Konov, V. I., Prokhorov, A. M., and Fedorov, V. B., "Laser Spark in a Slow Deflagration Regime," *Zhurnal Eksperimenticheskoy i Teoreticheskoy Fiziki Pisma Redaktorovanie*, Vol. 9, 1969, p. 665.

[6]Raizer, Y. P., "Subsonic Propagation of a Light Spark and Threshold Conditions to Maintain Plasma by Radiation," *Zhurnal Eksperimental'noi i Teoreticheskoi Fiziki*, Vol. 58, 1970, p. 2127.

[7]Jones, L. W., and Keefer, D. R., "Laser-Propulsion Project," *Astronautics and Aeronautics*, Vol. 20, 1982, p. 66.

[8]Glumb, R. J., and Krier, H., "Concepts and Status of Laser-Supported Rocket Propulsion," *Journal of Spacecraft and Rockets*, Vol. 21, 1984, p. 70.

[9]Krier, H., Mazumder, J., Rockstrah, T., Bender, T., and Glumb, R., "Continuous Wave Laser Gas Heating by Sustained Plasma in Flowing Argon," *AIAA Journal*, Vol. 24, 1986, p. 1656.

[10]Keefer, D., Welle, R., and Peters, C., "Power Absorption in Laser-Sustained Argon Plasmas," *AIAA Journal*, Vol. 24, 1986, p. 1663.

[11]Welle, R., Keefer, D., and Peters, C., "Laser-Sustained Plasmas in Forced Argon Convective Flow. Part 1. Experimental Studies," *AIAA Journal*, Vol. 25, 1987, p. 1093.

[12]Jeng, S.-M., Keefer, D., Welle, R., and Peters, C., "Laser-Sustained Plasmas in Forced Convective Argon Flow. Part 2. Comparison of Numerical Model with Experiment," *AIAA Journal*, Vol. 25, 1987, p. 1224.

[13]Jeng, S.-M., and Keefer, D., "Theoretical Estimation of Laser-Plasma Thruster Performances," *Journal of Propulsion and Power*, Vol. 5, 1989, p. 577.

[14]Steverding, B., "Subsonic Plasma Motion in Continuous Laser Light," *Journal of Physics D: Applied Physics*, Vol. 5, 1972, p. 1824.

[15]Raizer, Y. P., "One-Dimensional Linearized Model of Processes in Optical Plasmatron," *Kvantovaya Electronica*, Vol. 11, 1984, p. 64.

[16]Raizer, Y. P., and Surzhikov, S. T., "Numerical Analyses of the Processes in Optical Plasmatron," *Kvantovaya Electronica*, Vol. 11, 1984, p. 2301.

[17]Raizer, Y. P., and Surzhikov, S. T., "Numerical Analyses of One-Dimensional Continuous Optical Discharge in Atmospheric Air," *Teplofizika Vysokikh Temperatur*, Vol. 23, 1985, p. 30.

[18]Raizer, Y. P., and Silant'ev, A. Y., "Two-Dimensional Calculations of the Temperature Field of a Continuous Optical Discharge in Air," *Kvantovaya Electronica*, Vol. 13, 1986, p. 593.

[19]Raizer, Y. P., Silant'ev, A. Y., and Surzhikov, S. T., "Two-Dimensional Calculations of Continuous Optical Discharge in Atmospheric Air Flow," *Teplofizika Vysokikh Temperatur*, Vol. 25, 1987, p. 454.

[20]Raizer, Y. P., and Surzhikov, S. T., "Continuous Optical Discharge at Increased Pressures," *Kvantovaya Electronica*, Vol. 15, 1988, p. 551.

[21]Raizer, Y. P., and Surzhikov, S. T., "Continuous Optical Discharge Under the Conditions of Heat Gravitational Convection," *Mekh, Jidkost i Gas*, Vol. 4, 1989, p. 124.

[22]Gus'kov, K. G., Raizer, Y. P., and Surzhikov, S. T., "Observed Velocity of Slow Motion of an Optical Discharge," *Kvantovaya Electronica*, Vol. 17, 1990, p. 937.

[23]Surzhikov, S. T., "Numerical Modeling of a Low-Combustion Wave in CO_2 Laser's Beam," *Mathematical Modeling, Monthly Journal*, Vol. 2, 1990, p. 85.

[24]Surzhikov, S. T., "Radiative-Convective Heat Transfer in an Optical Plasmatron," *Teplofizika Vysokikh Temperatur*, Vol. 28, 1990, p. 1205.

[25]Gladush, G. G., Mamzer, A. P., and Yavochin, A. N., "Two-Dimensional Calculations of Continuous Optical Discharge," *Fizika Plazmy*, Vol. 11, 1985, p. 236.